◆ Human Brain Mapping 22:246–260(2004) ◆

Autoradiographic Distribution of Serotonin Transporters and Receptor Subtypes in Human Brain

Katarina Varnäs, Christer Halldin, and Håkan Hall*

Karolinska Institutet, Department of Clinical Neuroscience, Psychiatry Section, Karolinska Hospital, Stockholm, Sweden

Abstract: Several neurochemical in vitro and in vivo imaging studies have been aimed at characterizing the localization of serotonin receptors and transporters in the human brain. In this study, a detailed comparison of the distribution of a number of 5-HT receptor subtypes and the 5-HT transporter was carried out in vitro using human postmortem brain tissue. Anatomically adjacent whole hemisphere sections were incubated with specific radioligands for the 5-HT_{1A}, 5-HT_{1B}, 5-HT_{2A}, 5-HT_4 receptors and the 5-HT transporter. The autoradiograms revealed different laminar and regional distribution patterns in the isocortex, where 5-HT_{1A} and 5-HT_4 receptor binding showed highest densities in superficial layers and 5-HT_{2A} receptor binding was most abundant in middle layers. In cortical regions, 5-HT transporters were concentrated to several limbic lobe structures (posterior uncus, entorhinal, cingulate, insular and temporal polar regions). 5-HT_{1A} receptor densities were also high in limbic cortical regions (hippocampus, posterior entorhinal cortex, and subcallosal area) compared to the isocortex. Subregionally different distribution patterns were observed in the basal ganglia with a trend toward higher levels in ventral striatal (5-HT_{1B} receptors) and pallidal (5-HT transporters and 5-HT_{1B} receptors) regions. The localization in regions belonging to limbic cortico-striato-pallido-thalamic circuits is in line with the documented role of 5-HT in modulation of mood and emotion, and the suggested involvement of this system in pathophysiology of various psychiatric disorders. The qualitative and quantitative information reported in this study might provide important complements to in vivo neuroimaging studies of the 5-HT system. *Hum. Brain Mapp. 22:246–260, 2004.*

Key words: serotonin transporter; 5-HT_{1A} receptor; 5-HT_{1B} receptor; 5-HT_{2A} receptor; 5-HT_4 receptor; whole hemisphere autoradiography

INTRODUCTION

The serotonin (5-HT) system is distributed widely throughout the brain [Baumgarten and Grozdanovic, 1997] and mediates its various effects through at least 14 different receptor subtypes [Hoyer et al., 2002]. The 5-HT system is one of the main targets for pharmacologic treatment of several psychiatric disorders. Knowledge of the detailed distribution of different 5-HT receptor subtypes in human brain is therefore important in understanding the cause of psychiatric disorders and for development of psychoactive drugs. Furthermore, this information could reveal important knowledge on the interaction between human brain 5-HT receptor subtypes. Selective serotonin reuptake inhibitors (SSRIs) are used in the treatment of depression and several

Contract grant sponsor: Human Brain Informatics, Karolinska Institutet; Contract grant sponsor: Swedish Medical Research Council; Contract grant number: 11640; Contract grant sponsor: National Institute of Mental Health; Contract grant number: MH 44814-13.

*Correspondence to: Dr. Håkan Hall, Department of Clinical Neuroscience, Psychiatry Section, Karolinska Hospital, S-17176 Stockholm, Sweden. E-mail: hakan.hall@ks.se

Received for publication 13 June 2003; accepted 20 January 2004

DOI 10.1002/hbm.20035

Published online in Wiley InterScience (www.interscience.wiley.com).

other conditions, including obsessive-compulsive disorder and panic disorder [Nutt et al., 1999]. 5-HT_2 receptors have attracted interest as potential pharmacologic targets for the treatment of schizophrenia, due mainly to the findings that some atypical antipsychotics show high 5-HT_2 to D_2 receptor affinity ratio, relative to typical antipsychotic drugs [Meltzer et al., 1989]. The 5-HT_{1A} receptor partial agonist buspirone is used clinically in treatment of generalized anxiety disorder [Sramek et al., 2002], whereas there is evidence that 5-HT_{1A} receptor antagonists may potentiate the antidepressant effect of SSRIs [Artigas et al., 1996].

Less is known concerning the clinical pharmacology of central 5-HT_{1B} and 5-HT_4 receptors. Preclinical data suggest that 5-$HT_{1B/1D}$ receptors may be involved in depression and anxiety disorders, and that selective receptor antagonists could potentially be useful for treatment of these conditions [for review, see Moret and Briley, 2000]. Mutant mice lacking the 5-HT_{1B} receptor are more aggressive compared to wild-type mice in the resident–intruder aggression model [Saudou et al., 1994]. Increased alcohol consumption [Crabbe et al., 1996] and increased vulnerability to cocaine [Rocha et al., 1998] have also been reported for 5-HT_{1B} receptor knockout mice. The distribution pattern in combination with neurochemical and behavioral observations have indicated that brain 5-HT_4 receptors may be involved in cognition and anxiety [Eglen, 1997].

Abnormalities in the 5-HT system have been found in different psychiatric conditions. In several cortical regions of postmortem schizophrenic brains, there have been reports on increased density of 5-HT_{1A} receptors [for review, see Bantick et al., 2001] and reduced densities of 5-HT_{2A} receptors [for review, see Dean, 2003]. Increased cortical densities of 5-HT_{1A} receptors in schizophrenia have been demonstrated also in a recent positron emission tomography (PET) study [Tauscher et al., 2002]. In vivo imaging studies have reported reduced levels of brain 5-HT transporters [Malison et al., 1998] and 5-HT_{1A} receptors [Drevets et al., 1999; Sargent et al., 2000] in depression. Several abnormalities in serotonergic binding sites have been demonstrated in suicide victims, such as reduced levels of 5-HT transporters and increased levels of 5-HT_{1A} receptors [Arango et al., 1995] in the ventrolateral prefrontal cortex, and increased 5-HT_{2A} receptor binding in the prefrontal cortex [see Arango et al., 1997].

The availability of selective, high-affinity radioligands for 5-HT_{1A} receptors [Pike et al., 1996], 5-HT_{2A} receptors [Ito et al., 1998], 5-HT_4 receptors [Pike et al., 2003], and the 5-HT transporter [Szabo et al., 1995] enables characterization of binding site localization in vivo using PET or single photon emission tomography (SPECT). Autoradiography on postmortem human brain whole hemisphere cryosections provides high-resolution images and is therefore a suitable technique for detailed description of receptor distribution [Hall et al., 1998]. Such autoradiographic images may serve as high-resolution anatomic correlates for lower resolution PET and SPET receptor studies.

The localization patterns of the 5-HT receptor subtypes are different, but show some common regional distribution. For instance, several subtypes are localized in cerebral cortex and basal ganglia. Although the distribution of each receptor subtype (5-HT_{1A}, 5-HT_{1B}, 5-HT_{2A}, and 5-HT_4) has been presented previously [Bonaventure et al., 2000; Hall et al., 1997, 2000; Pazos et al., 1987a,b; Varnäs et al., 2001, 2003], no detailed comparison of regional and subregional localization using adjacent sections of human brain tissue has been undertaken to analyze these binding sites.

The purpose of this work was to compare the detailed regional and subregional anatomic distribution of different 5-HT binding sites. The distribution pattern was compared for four of the main G-protein coupled 5-HT receptor subtypes and the 5-HT transporter in adjacent human brain sections. Labeling of 5-HT_{1A} and 5-HT_{2A} receptors was carried out using the highly selective and potent radioligands [^{3}H]WAY-100635 [Khawaja et al., 1995] and [^{3}H]M100907 [Kehne et al., 1996], respectively. The 5-$HT_{1B/1D}$ radioligand [^{3}H]GR 125743 [Doménech et al., 1997] was used to study the distribution of 5-HT_{1B} receptors in the presence of a selective 5-HT_{1D} antagonist, and 5-HT_4 receptor autoradiography was performed using the selective radioligand [^{125}I]SB 207710 [Brown et al., 1993]. The 5-HT transporter radioligand [^{3}H]citalopram was used to study distribution of the 5-HT transporter in the human brain. Whole hemisphere cryosections were used to enable a complete mapping of binding site distribution, special emphasis was put on forebrain areas rich in 5-HT innervation, such as limbic cortices [for definition, see Heimer, 2003] and basal ganglia.

MATERIALS AND METHODS

Compounds

[^{3}H]Citalopram (*N*-methyl-[^{3}H]-citalopram, specific radioactivity 85 Ci/mmol) was obtained from NEN Life Science Products (Boston, MA). Radiosynthesis of [^{3}H]WAY-100635[1] was carried out as described previously [Österlund et al., 2000] using *O*-desmethyl-WAY-100635 and [^{3}H]methyl iodide, in a solution containing dimethylformamide and sodium hydroxide (5 M). The radioligand (specific radioactivity, 55 Ci/mmol) was purified on a reverse phase high-performance liquid chromatography (HPLC) column, evaporated and diluted in 75% ethanol. [^{3}H]GR 125743, specific radioactivity 74.0 Ci/mmol, was obtained from Amersham Pharmacia Biotech, Uppsala. [^{3}H]M100907[2] was prepared from the 3-hydroxy precursor (MDL 105725) as described previously using [^{3}H]methyl iodide, in a solution containing acetone and sodium hydroxide (5M). The radioligand (specific radioactivity, 46 Ci/mmol) was purified on a normal-phased HPLC column, evaporated and dissolved

[1] *O*-methyl-[^{3}H]-*N*-(2-[4-(2-methoxyphenyl)-1-piperazinyl]ethyl)-*N*-(2-pyridinyl)cyclohexanecarboxamide trihydrochloride

[2] 3-*O*-methyl-[^{3}H](*R*)-(+)-4-(1-hydroxy-1-[2,3-dimethoxyphenyl]-methyl)-*N*-2-(4-fluorophenylethyl)piperidine

TABLE I. Demographic data and description of brains used

Patient no.	Age (yr)	Hemisphere	Gender	Postmortem time (hr)	Cause of death
46	63	Left	M	48	Myocardial infarction
62	53	Right	M	15.3	Myocardial infarction
70	61	Left	M	15.4	Heart failure
71	55	Right	M	29	Myocardial infarction
73	58	Left	F	6	Myocardial infarction

The number of levels studied per brain for each binding site were three for Patient 46, 1 for Patient 62, and two for the other three subjects.

in 70% ethanol. [^{125}I]SB 207710[3] was prepared according to Pike et al. [2003] from the precursor SB 207715 ([1-*n*-butyl-4-piperidinyl]methyl-8-amino-7-tributylstannyl-1,4-benzodioxane-5-carboxylate). SB 207715 was incubated in [^{125}I]sodium iodide solution (no carrier added) in the presence of chloramine-T. The radioligand (specific radioactivity, 2,200 Ci/mmol) was purified on a reverse phase column, evaporated and dissolved in 75% ethanol. The radiochemical yield was 60% and the radiochemical purity was over 99%. Formulated [^{125}I]SB 207710 was radioactively stable during the period of investigation.

The selective 5-HT$_{1D}$ receptor ligand, PNU-142633, was kindly provided by Dr. K. Svensson (Pharmacia Corp., Kalamazoo, MI). Other compounds and chemicals were obtained from commercially available sources and were of analytical grade wherever possible.

Brain Tissue

Human brains were obtained postmortem at clinical autopsy at the National Institute of Forensic Medicine, Karolinska Institutet (Stockholm, Sweden). The study was approved by the Ethics Committee at Karolinska Institutet and the Swedish Board of Social Welfare. Whole hemispheres (see Table I for details) were removed, frozen, and cryosectioned as described previously [Hall et al., 1998, 2001], using a heavy-duty cryomicrotome (Leica cryomacrocut CM3600, Leica, Nussloch, Germany). Tissue was obtained from five control subjects with no documented history of neurologic, psychiatric, or substance abuse disorders. From examination at autopsy and during sectioning, none of the brains exhibited damages, abnormalities, or neurologic features. The whole hemispheres were oriented so that a line connecting the anterior and posterior commissures was parallel to the surface of the cryostat specimen holder. The tissue cryosections (thickness 100 μm) were transferred to gelatinized or poly-L-lysine treated glass plates (10 × 22 cm), dried at room temperature, and then stored with dehydrating agents (−25°C) until use.

[3](1-*n*-butyl-4-piperidinyl) methyl-8-amino-7-[^{125}I]iodo-1,4-benzodioxane-5-carboxylate

Autoradiography

The autoradiographic experiments were carried out essentially as described previously [Hall et al., 1997, 2001]. Incubations and preincubations (see Table II for detailed protocols) were carried out at room temperature in Tris-HCl or phosphate buffers (pH 7.4; total volume about 14 ml). Washing was carried out with cold (4°C) buffer, followed by a brief cold wash by dipping the sections into distilled water. The sections were dried on a warm plate and stored with dehydrating agents. For each level, adjacent cryosections were stained with cresyl violet and used as anatomic correlates.

For the tritiated radioligands, detection and quantification was carried out using phosphor imager analysis (scanner, Fuji BAS-15000 image reader; imaging plates, BAS IP-TR 2040; Fuji Photo Film, Japan; 1 week exposure). When required, background scans obtained after 1-week exposure were subtracted from the images using Science Lab 98, L Process 1.72 to eliminate possible remaining background from previous exposures. Image Gauge 3.12 (Fuji Photo Film) was used for the image densitometry. Measurements were performed in images representing total and nonspecific binding, respectively, for each brain region of interest. Photostimulated luminescence (PSL)/mm^2 values obtained were transformed into radioactivity values and to binding density (pmol/g tissue, original wet weight) using ^{3}H-calibrating scales (Microscales, Amersham, UK and American Radiolabeled Chemicals Inc., St. Louis, MO). Specific binding densities were calculated by subtracting the level of non-specific binding (for specific blocking compounds, see Table II) from the total binding for each radioligand and brain region.

[^{125}I]SB 207710 autoradiograms were obtained using film exposure (see below for description). Quantitative determinations of [^{125}I]SB 207710 binding were obtained by transforming the measured pixel gray levels into binding densities (pmol/g tissue) using ^{125}I-calibrating scales (Microscales; Amersham, UK). Density values were adjusted for section thickness by dividing obtained values by 5, as there is a linear relationship between section thickness and radiation at the surface of tissue for section thickness up to 100 μm [Varnäs and Hall, unpublished observations]. Measurements were carried out using Adobe Photoshop 6.0. The specific binding was calculated by

TABLE II. Study protocol for autoradiographic experiments

Receptor/ transporter	Radioligand	Conc.	Incubation buffer	Preincubation (min)	Incubation (min)	Washing (min)	Definition of nonspecific binding	References
5-HT transporter	[^{3}H]Citalopram	2nM	10.14 mM Na_2HPO_4 137 mM NaCl 2.7 mM KCl 1.76 mM KH_2PO_4	15	90	3 × 10	10 μM fluoxetine	Mantere et al., 2002
5-HT_{1A}	[^{3}H]WAY-100635	2nM	50 mM Tris 2 mM $CaCl_2$	2 × 15	60	2 × 10	10 μM 8-OH-DPAT	Hall et al., 1997
5-HT_{1B}	[^{3}H]GR 125743	2nM	170 mM Tris 4 mM $CaCl_2$ 0.1% ascorbic acid 10 μM pargyline 800 nM PNU-142633	2 × 15	90	3 × 10	10 μM 5-HT	Varnäs et al., 2001
5-HT_{2A}	[^{3}H]M100907	2nM	50 mM Tris 0.1% ascorbic acid 120 mM NaCl 5 mM KCl 2 mM $CaCl_2$ 1 mM $MgCl_2$		60	3 × 5	10 μM ketanserin	Hall et al., 2000
5-HT_4	[^{125}I]SB 207710	17pM	50 mM Tris 5 mM $MgCl_2$ 1 mM EGTA 10 μM pargyline		60	3 × 10	10 μM 5-HT	Patel et al., 1995

subtracting nonspecific binding (for definition, see Table II) from the total [^{125}I]SB 207710 binding.

For visualization and image presentation, autoradiographic films (Kodak BioMax MR; Eastman Kodak Company, Rochester, NY or ^{3}H-Hyperfilm; Amersham, UK) were applied to the sections. Exposure times were 4 days for [^{125}I]SB 207710 and 10–13 weeks for the [^{3}H]-labeled radioligands. After development (developer, Kodak D19; fixation, Kodak Fixer 3000), autoradiograms were digitized using a high-resolution scanner (ScanMaker E6; Microtek) and Adobe Photoshop 5.0 or 6.0. Adobe Photoshop 6.0 was used for processing of the images. The images show total binding (except for Fig. 2G–K), as the level of nonspecific binding is low for all the radioligands used.

RESULTS

General

General distribution patterns have been described previously for each binding site [Gurevich and Joyce, 1996; Hall et al., 1997, 2000; Mantere et al., 2002; Pazos et al., 1987a,b; Varnäs et al., 2001, 2003]. In Figure 1, the binding patterns of different 5-HT binding sites were compared in adjacent cryosections of human brain whole hemispheres. As expected, the distribution pattern varied markedly between the different binding sites. In general, [^{3}H]citalopram binding to the 5-HT transporter, [^{3}H]GR 125743 binding to the 5-HT_{1B} receptor, and [^{125}I]SB 207710 binding to the 5-HT_4 receptor were most abundant in subcortical structures, whereas [^{3}H]WAY-100635 and [^{3}H]M100907 binding to 5-HT_{1A} and 5-HT_{2A} receptors, respectively, were concentrated to the cerebral cortex. As described previously [Hall et al., 1997, 2000; Mantere et al., 2002; Varnäs et al., 2001, 2003], and as illustrated in Figure 2G–K, the level of nonspecific binding was relatively low and homogeneous for [^{3}H]citalopram, [^{3}H]GR 125743, and [^{125}I]SB 207710 (Fig. 2G, I, and K, respectively), and was very low for [^{3}H]WAY-100635 and [^{3}H]M100907 (Fig. 2H and 2J, respectively). Binding densities for the different 5-HT binding sites are presented in Table III.

Limbic Cortices

In the following section and in Table III, limbic cortical areas are defined according to Heimer et al. [2003]. [^{3}H]Citalopram binding was higher in the cingulate gyrus compared to that in isocortical regions and was higher in superficial layers compared to that in internal layers. Within the cingulate cortex, the highest levels were seen in the subcallosal area followed by the anterior cingulate, and the binding was lowest in the posterior cingulate region (Fig. 2, Table III).

As is visualized in Figure 3, the studied 5-HT receptor binding sites showed subregionally different distribution patterns in the hippocampal formation. [^{3}H]Citalopram binding was low and distributed diffusely in the hippocampal body and was markedly higher in the posterior uncus. In the hippocampal body, higher levels were observed in CA3 compared to that in CA1–2. The binding was concentrated to the molecular layer of CA3 and in the dentate gyrus, with lower levels in the pyramidal cell layer of the CA regions (Fig. 3B). [^{3}H]WAY-100635 binding to the 5-HT_{1A} receptor was very high (specific binding, 123 pmol/g) in the pyramidal cell layer and lower in the molecular layer (stratum lacunosum moleculare, 85 pmol/g) of CA1–2 with lower levels in the CA3 field. The binding was high in the molec-

ular cell layer and lower in the granular cell layer of the dentate gyrus (Fig. 3C). The specific [^{3}H]GR 125743 binding was low throughout the hippocampal formation, with highest intensities in the subiculum and the molecular layer (probably corresponding to the stratum lacunosum-moleculare, 14 pmol/g) of Ammon's horn (Fig. 3D). [^{3}H]M100907 binding was concentrated in the CA1–2 field (27 and 24 pmol/g in the pyramidal and molecular cell layer, respectively) and was markedly lower in the CA3 region, dentate gyrus, and subiculum (Fig. 3E). [^{125}I]SB 207710 binding to the 5-HT$_4$ receptor showed the highest levels in the pyramidal cell layer of CA1 and subiculum with lower levels in the CA3 region. In the subiculum, the specific [^{3}H]citalopram, [^{3}H]WAY-100635, and [^{3}H]GR 125743 binding sites were concentrated to the most external part of the pyramidal layer, whereas [^{125}I]SB 207710 binding sites were distributed throughout the entire pyramidal cell layer of the subicular cortex.

The entorhinal cortex was partitioned into three subregions based on the distinct distribution patterns of the [^{3}H]citalopram, [^{3}H]WAY-100635, and [^{3}H]M100907 binding sites (Fig. 4, Table III). High levels of [^{3}H]citalopram binding were observed in external layers of the entorhinal cortex (Fig. 4B). The binding was higher in anterior compared to posterior subregion. [^{3}H]WAY-100635 binding was equally high in external and internal layers of the anterior entorhinal cortex. The highest densities were found in external layers of the posterior subregion of the entorhinal cortex. [^{3}H]M100907 binding was markedly lower in the entorhinal cortex compared to other cortical regions. [^{3}H]GR 125743 binding was distributed homogeneously, with no evident subregional differences, although a trend toward higher binding could be identified in external as compared to internal layers and in anterior as compared to posterior regions (Fig. 4D).

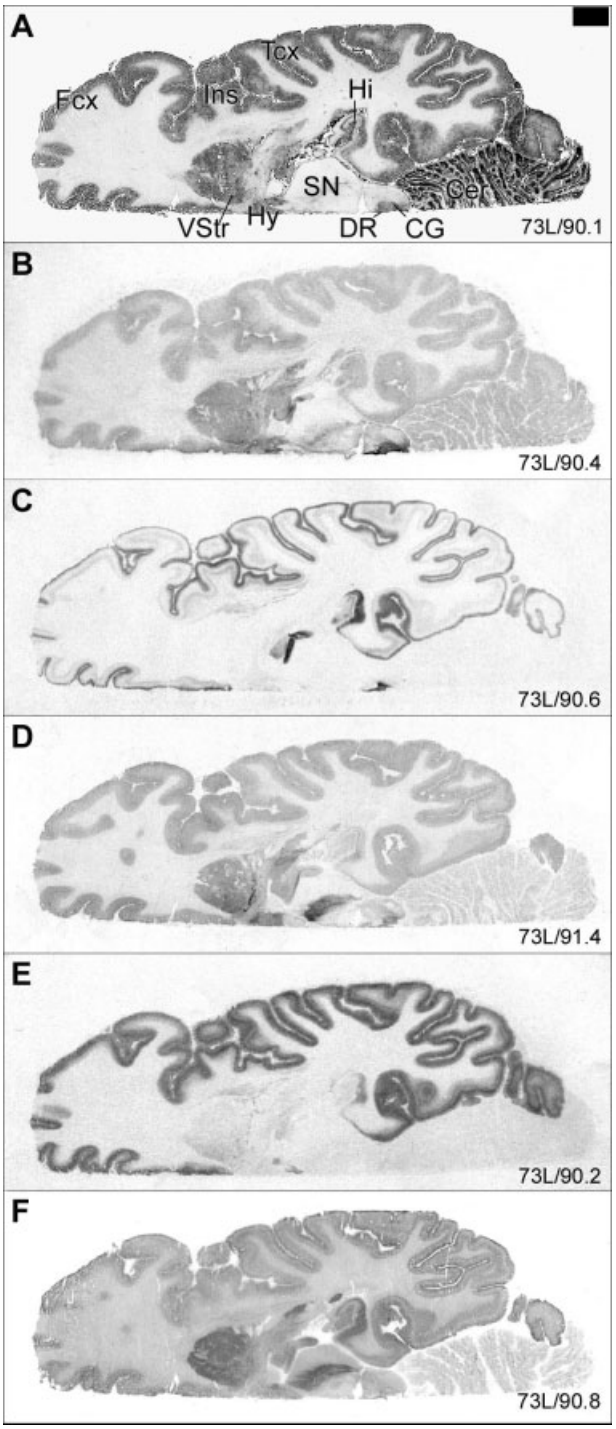

Figure 1.

Whole hemisphere autoradiograms comparing the distribution of the 5-HT transporter and receptor binding sites in human brain cryosections. The following information and the abbreviation list apply to all images: Total binding is shown for the different radioligands. **A:** Cresyl violet-stained section. **B:** [^{3}H]Citalopram binding to the 5-HT transporter. **C:** [^{3}H]WAY-100635 binding to the 5-HT$_{1A}$ receptor. **D:** [^{3}H]GR 125743 binding to the 5-HT$_{1B}$ receptor in the presence of the 5-HT$_{1D}$ antagonist PNU-142633 (800 nM). **E:** [^{3}H]M100907 binding to the 5-HT$_{2A}$ receptor. **F:** [^{125}I]SB 207710 binding to the 5-HT$_4$ receptor.[4] Numbers in the lower right corner represent internal brain number and distance (mm) from the vertex. Scale bar = 10 mm. ACG, anterior cingulate gyrus; Amg, amygdala; ATh, anterior thalamus; Ca, caudate nucleus; CA1–3, Ammon's horn; Cer, cerebellum; CG, central gray; DG, dentate gyrus; DR, dorsal raphe nucleus; Ent, entorhinal cortex; Hi, hippocampus; Hy, hypothalamus; Fcx, frontal cortex; Ins, insular cortex; LP, lateral posterior thalamus; MD, mediodorsal thalamus; MnR, median raphe nucleus; Pu, putamen; Pul, pulvinar; R, red nucleus; S, subiculum; SCA, subcallosal area; SN, substantia nigra; Tcx, temporal cortex; TmP, temporal pole; Un, posterior uncus; VA, ventral anterior thalamus; VL, ventral lateral thalamus; VStr, ventral striatum. [4Figure 1F reprinted from K. Varnäs, C. Halldin, V.W. Pike, H. Hall (2003): Distribution of 5-HT$_4$ receptors in the postmortem human brain—an autoradiographic study using [^{125}I]SB 207710. *European Neuropsychopharmacology* 13:228–234. Reproduced with permission from Elsevier.]

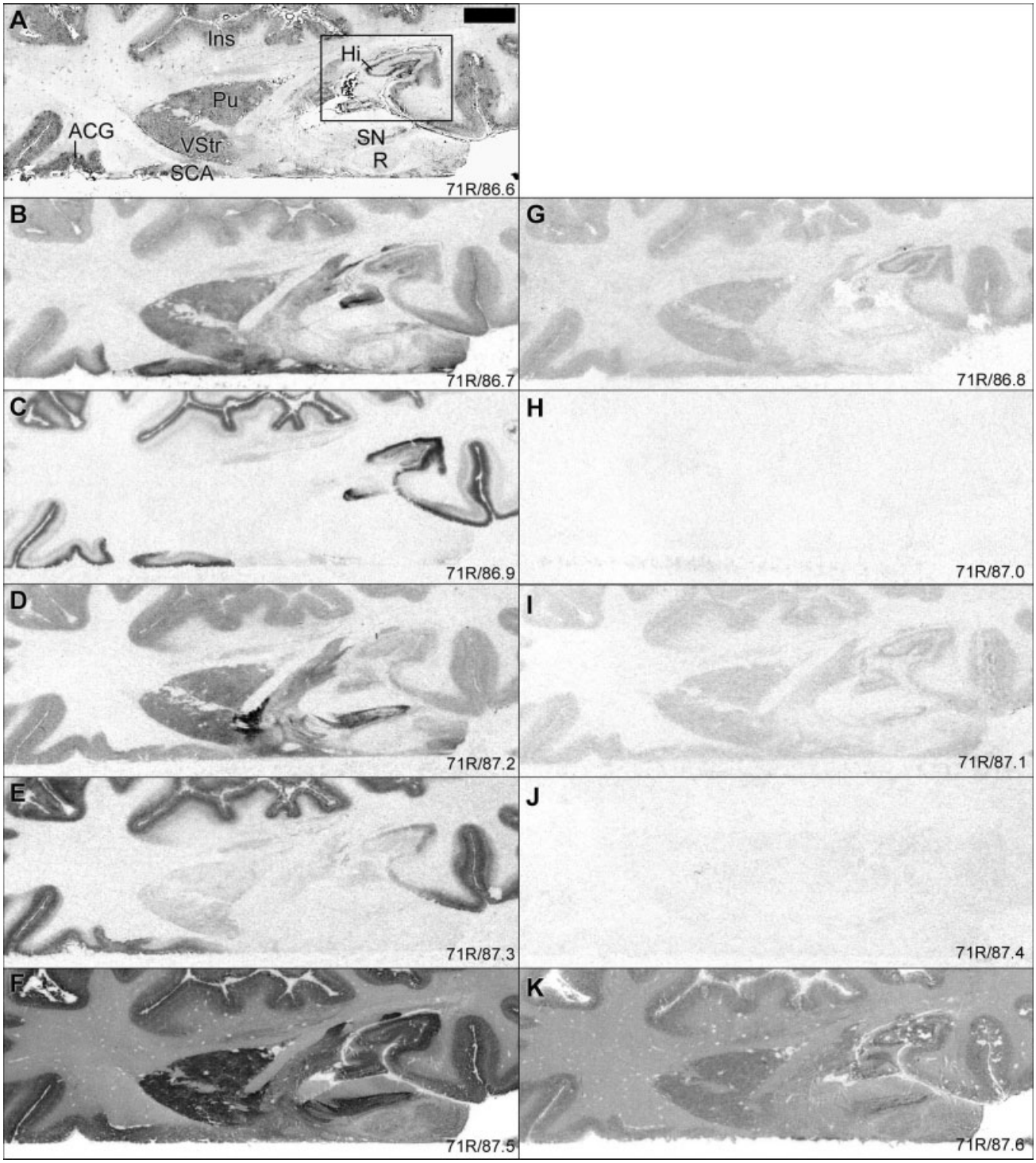

Figure 2.

Autoradiograms comparing distribution of 5-HT binding sites in limbic cortices (for definition, see Heimer, 2003), ventral striatum, and midbrain. G–K: Shows level of nonspecific binding for each radioligand. For general figure information see legend to Figure 1. Square (A) shows location of image section magnified in Figure 3.

TABLE III. Autoradiographic distribution of 5-HT binding sites in the human brain

		[^{3}H]Citalopram		[^{3}H]WAY-100635		[^{3}H]GR 125743		[^{3}H]M100907		[^{125}I]SB 207710	
Brain region	n	Mean	SD	Mean	SD	Mean	SD	Mean	SD	Mean	SD
Limbic cortices											
Hippocampus CA1–2, pyramidal layer	7 (5)	2.6	1.7	123	21	3.7	2.5	27	10	0.32	0.11
CA1–2, molecular layer	7 (5)	8.4	3.9	85	19	13	5.4	24	7.3	0.23	0.098
Dentate gyrus	6 (4)	6.8	3.4	52	12	3.9	2.6	8.1	3.2	0.19	0.073
Posterior uncus	2 (2)	31	(22, 39)	108	(92, 124)	10	(9.7, 11)	13	(9.1, 17)	0.19	(0.15, 0.22)
Amygdala (basolateral complex)	3 (3)	11	4.3	13	5.5	12	2.1	37	3.2	0.19	0.084
Anterior cingulate gyrus											
External layers	7 (4)	20	2.8	71	3.0	19[a]	4.4	55	8.0	0.19	0.055
Internal layers	7 (4)	10	2.3	19	2.8	18[a]	3.6	25	3.9	0.16	0.039
Posterior cingulate gyrus											
External layers	2 (2)	8.7	(7.7, 9.8)	43	(36, 50)	16	(15, 16)	55	(51, 59)	0.18	(0.13, 0.22)
Internal layers	2 (2)	4.1	(0.0, 8.2)	11	(10, 11)	9.9	(9.4, 10)	24	(24, 24)	0.14	(0.12, 0.16)
Subcallosal area											
External layers	3 (3)	43	17	90	9.7	15[a]	(11, 20)	55	11	0.13	0.017
Internal layers	3 (3)	26	14	31	6.1	15[a]	(12, 19)	27	6.9	0.14	0.0086
Entorhinal cortex											
Anterior, external layers	3 (3)	36	3.1	73	15	19	4.3	24	6.4	0.26	0.090
Anterior, internal layers	3 (3)	13	2.6	73	21	13	4.4	24	0.88	0.26	0.089
Middle, external layers	3 (3)	18	6.3	66	18	19	5.9	23	2.2	0.18	0.059
Middle, internal layers	3 (3)	7.3	0.74	38	17	10	6.4	21	3.3	0.22	0.065
Posterior, external layers	3 (3)	15	2.0	88	21	11	2.2	57	14	0.22	0.10
Posterior, internal layers	3 (3)	7.9	1.4	27	8.2	11	3.5	36	8.6	0.18	0.084
Insular cortex											
External layers	7 (4)	12	3.2	73	6.7	18	3.0	60	7.4	0.18	0.043
Middle layers	7 (4)	7.8	3.3	14	4.2	19	3.1	61	9.0	0.12	0.045
Internal layers	7 (4)	5.3	1.9	18	4.2	16	3.9	30	4.5	0.12	0.024
Temporal polar cortex											
External layers	3 (3)	17	4.6	97	25	16	1.7	67	11	0.31	0.15
Internal layers	3 (3)	8.1	2.0	23	3.9	17	1.5	36	12	0.24	0.11
Isocortex											
Frontal cortex											
External layers	7 (4)	5.4	2.2	54	8.0	20	2.6	56	13	0.18	0.066
Middle layers	7 (4)	4.1	1.4	9.3	2.2	20	2.6	59	13	0.11	0.037
Internal layers	7 (4)	3.4	1.4	11	1.6	16	2.7	30	4.6	0.12	0.031
Temporal cortex											
External layers	6 (5)	5.2	3.3	68	15	14	3.2	62	7.8	0.26	0.095
Middle layers	6 (5)	3.3	2.1	9.6	1.0	14	3.3	60	10	0.14	0.069
Internal layers	6 (5)	1.8	1.5	12	3.1	11	2.7	35	6.3	0.18	0.061
Occipital cortex (BA17)											
External layers	4 (3)	3.2	2.1	23	5.1	21	3.0	56	13	0.12	0.027
Middle layers	4 (3)	4.4	3.8	3.0	0.60	34	3.7	55	9.2	0.039	0.015
Internal layers	4 (3)	4.0	3.4	1.5	0.69	16	4.0	32	1.8	0.051	0.029
Striatum and pallidum											
Caudate nucleus	4 (4)	17	4.2	1.8	1.2	16	3.8	13	3.2	0.29	0.049
Putamen	4 (4)	9.8	2.6	1.1	0.70	8.9	3.4	5.4	2.5	0.24	0.021
Ventral striatum	3 (3)	19	3.6	2.8	2.0	35	8.7	16	3.0	0.26	0.029
Globus pallidus	3 (2)	4.0	1.4	<1	—	35	1.2	1.5	2.0	0.27	0.050
Ventral pallidum	2 (2)	15	(15, 15)	1.3	(0.37, 2.2)	82	(78, 86)	3.5	(2.9, 4.1)	0.33	(0.30, 0.36)
Thalamus											
Anterior	4 (4)	9.2	2.4	<1	—	<1	—	6.2	1.8	0.10	0.034
Mediodorsal	4 (4)	10	3.1	2.5	0.42	1.9	0.69	11	1.3	0.058	0.013
Pulvinar	4 (4)	13	3.2	1.7	0.92	2.8	1.2	7.0	2.0	0.081	0.021
Brainstem											
Substantia nigra	2 (2)	9.9	(7.7, 12)	<1	—	38	(30, 46)	4.5	(2.5, 6.5)	0.30	(0.29, 0.31)
Central gray area	6 (5)	56	17	12	6.8	27	6.0	5.6	3.4	0.11	0.039
Dorsal raphe nucleus	2 (2)	120	(108, 132)	140	(119, 161)	21	(18, 23)	6.3	(4.6, 8.0)	0.14	(0.13, 0.16)

Values are presented as specific binding and are expressed in pmol/g tissue, original wet weight; n denotes number of measurements followed by number of subjects in parenthesis. Mean and standard deviation (alternatively the two values where n = 2). For the [^{3}H]100907 binding, data from two brain sections are presented as total binding, as the level of nonspecific binding is very low for this radioligand [Hall et al., 2000]. All other data represent specific binding as obtained by subtraction of nonspecific binding from total binding in anatomically adjacent sections. Data for the frontal and temporal cortices are from the inferior and the middle gyrus, respectively. External, middle, and internal cortical layers roughly correspond to layers I–II, III–IV, and V–VI, respectively for the isocortical regions.

[a] n = 6 and 2 for [^{3}H]GR 125743 binding in the anterior cingulate gyrus and the subcallosal area, respectively (due to tissue destruction in one section).

In the basolateral amygdala (Fig. 4), [^{3}H]M100907 binding showed the highest density (37 pmol/g) of the binding sites examined. The density of [^{3}H]WAY-100635 binding sites was very low in the basolateral amygdala and was higher in the paralaminar nucleus.

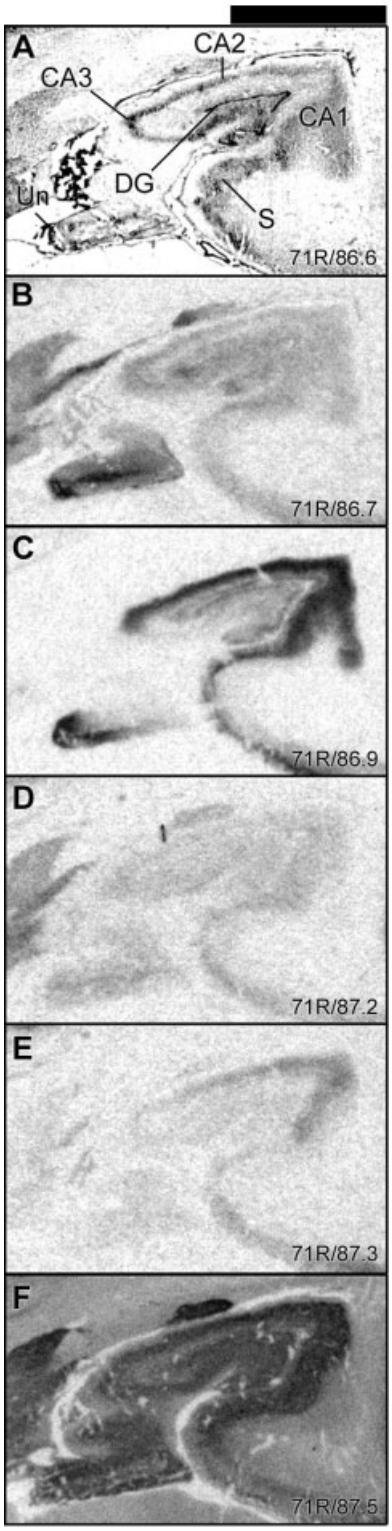

[^{3}H]Citalopram binding was higher in the temporal polar cortex compared to that in the isocortical temporal regions. [^{3}H]Citalopram binding was concentrated to the most external layers, whereas [^{3}H]WAY-100635 binding displayed a more widespread distribution with high levels in a wider superficial band (Fig. 4B,C, respectively).

In insular cortical regions, [^{3}H]citalopram binding was higher compared to that in isocortical regions, with a gradual decrease toward the internal cortical layers. [^{3}H]GR 125743 binding was distributed homogeneously with no clear laminar differences (Table III).

Isocortex

The isocortical binding was laminated for all 5-HT binding sites examined, and most prominent for [^{3}H]WAY-100635 and [^{3}H]M100907 binding (Fig. 1).

In general, [^{3}H]WAY-100635 binding was concentrated in two bands, one of very high intensity in superficial layers (I–II), and one band (corresponding to layer V–VI) displaying lower levels. The [^{3}H]M100907 binding was distributed in three bands, with the highest levels in middle layers (corresponding to layer III) and two bands corresponding to layers I and V. [^{3}H]Citalopram binding was low in isocortex and was highest in superficial layers (I–II). In most cortical regions, [^{3}H]GR 125743 binding was distributed homogeneously throughout the cortical laminae with slightly higher intensities in external compared to internal cortical layers. The [^{125}I]SB 207710 binding pattern roughly paralleled that for [^{3}H]WAY-100635, with the highest binding in external cortical layers, lower levels in deep layers, and the lowest intensity in middle cortical layers.

Subregionally different distribution patterns were observed in isocortical areas. In frontal cortex, [^{125}I]SB 207710 binding in deep cortical layers was restricted to one thin band, most likely corresponding to layer V (Fig. 5F). The most abundant binding sites in the occipital cortex (Fig. 6) corresponded to the 5-HT$_{1B}$ and 5-HT$_{2A}$ receptor subtypes. [^{3}H]M100907 binding showed the highest intensity in external layers and [^{3}H]GR 125743 binding was concentrated to a middle layer (probably corresponding to layer IV). The levels of [^{3}H]WAY-100635 and [^{125}I]SB 207710 binding sites were markedly lower in occipital cortex compared to that in other cortical regions.

Striatum and Pallidum

Intermediate levels of all examined binding sites were identified in caudate nucleus and putamen, except for

Figure 3.
Details of the autoradiograms in Figure 2 showing total binding of 5-HT binding sites in hippocampal formation including CA1–3 of Ammon's horn, dentate gyrus, and subiculum. For general figure information see legend to Figure 1.

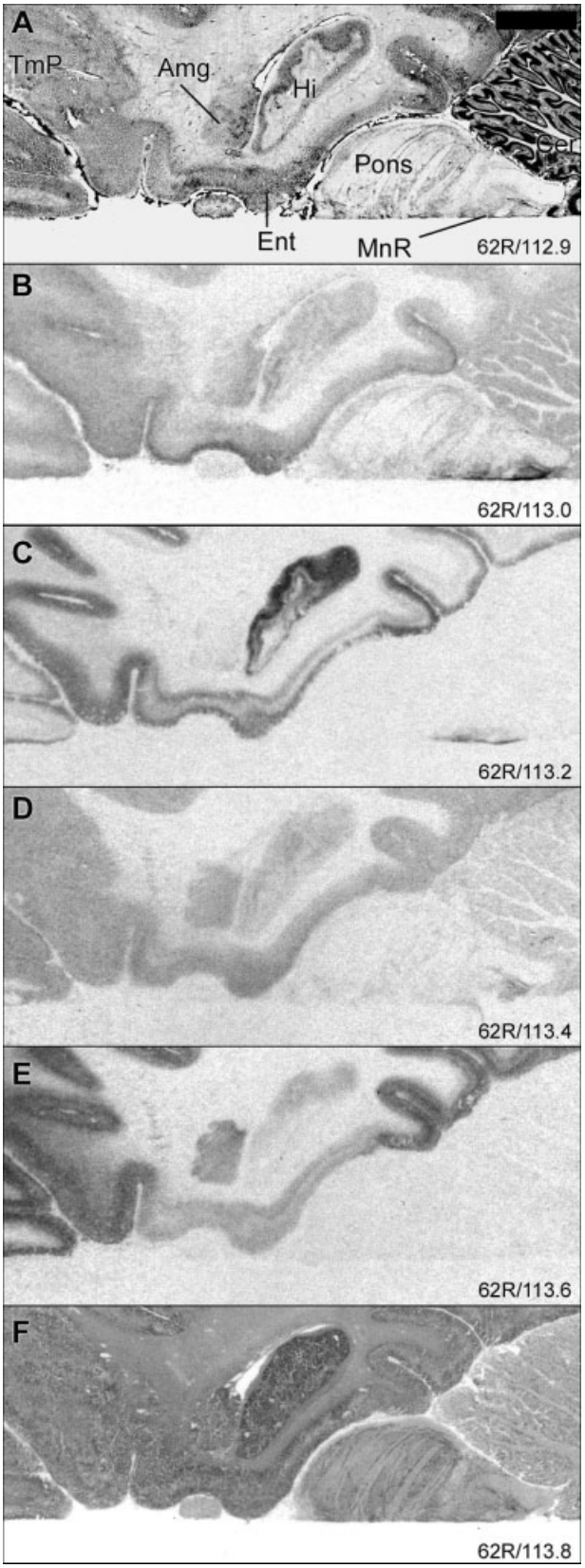

[^{3}H]WAY-100635 binding to the 5-HT$_{1A}$ receptor subtype, which was very low to absent in these regions (Fig. 7). All these binding sites displayed slightly higher levels in the caudate nucleus compared to that in the putamen. Subregional distribution patterns differed considerably for the different binding sites. [^{3}H]GR 125743 binding was higher in ventral as compared to dorsal striatal regions. [^{3}H]Citalopram, [^{3}H]M100907, and [^{125}I]SB207710 binding sites were distributed heterogeneously in caudate nucleus and putamen. [^{3}H]M100907 binding displayed a patchy distribution pattern. The 5-HT$_{2A}$ receptor binding sites have been reported previously to be confined to the striosome compartment, as defined by high densities of benzodiazepine binding sites and low acetylcholinesterase content [López-Giménez et al., 1999; Waeber and Palacios, 1994]. On the other hand, [^{125}I]SB207710 binding was high throughout caudate nucleus and putamen, except for low density binding patches. This distribution pattern did not overlap with the striosome matrix compartmentalization as visualized with [^{3}H]M100907. [^{3}H]Citalopram binding was heterogeneous in the striatum, with higher levels in restricted zones in medial caudate nucleus and lateral putamen. In ventral striatum, higher levels of [^{3}H]citalopram binding were found in medial as compared to lateral parts.

In globus pallidus, high densities of [^{3}H]GR 125743, comparatively high [^{125}I]SB207710 binding, and only low levels of [^{3}H]citalopram binding sites were detected. [^{3}H]WAY-100635 and [^{3}H]M100907 binding densities were very low or absent in the globus pallidus. [^{3}H]GR 125743 and [^{3}H]citalopram binding densities were considerably higher in the ventral pallidum compared to that in the globus pallidus.

Thalamus

[^{3}H]Citalopram binding was observed throughout several thalamic nuclei including the anterior, mediodorsal, midline, and pulvinar nuclei (Fig. 7). Very high levels (86 pmol/g) were observed in the midline nuclei, where dense [^{3}H]WAY-100635 binding (46 pmol/g) and intermediate levels of [^{3}H]GR 125743 binding (~21 pmol/g) were also observed. [^{3}H]WAY-100635 and [^{3}H]GR 125743 binding was low to absent in anterior, mediodorsal, and pulvinar nuclei. [^{3}H]M100907 binding was low in these nuclei and was concentrated to mediodorsal nucleus. [^{125}I]SB 207710 binding was highest in anterior and pulvinar nuclei. Intermediate levels of [^{3}H]WAY-100635 binding was detected in the intralaminar nuclei. All examined binding sites seemed to be very low to absent in lateral and ventral anterior nuclei.

Brainstem and Cerebellum

In general, [^{3}H]citalopram, [^{3}H]GR 125743, and [^{125}I]SB 207710 binding sites were widespread in the brainstem nu-

Figure 4.
Autoradiograms illustrating distribution of 5-HT binding sites at the level of pons. For general figure information see legend to Figure 1.

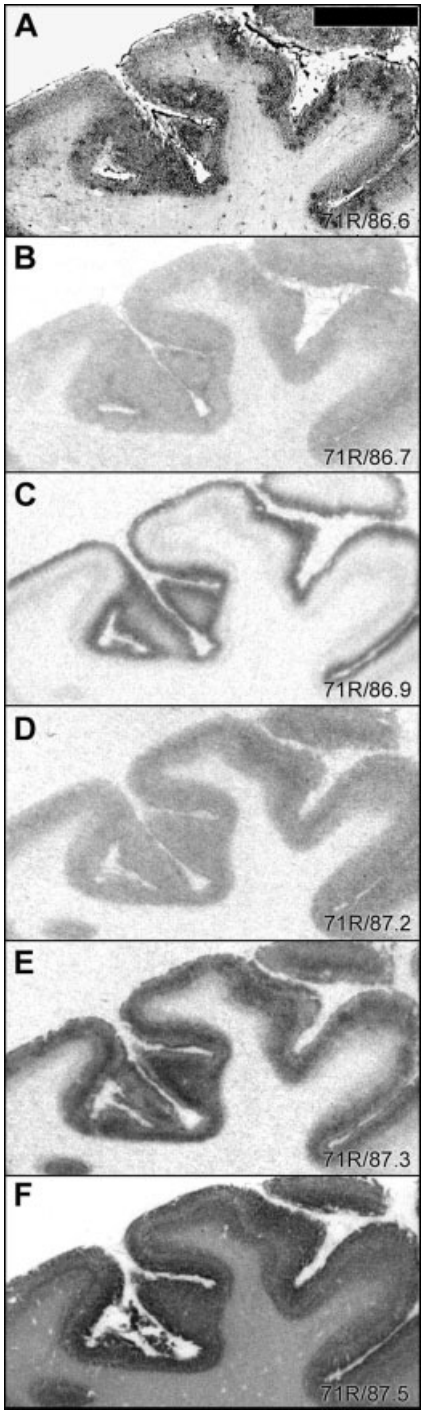

Figure 5.
Autoradiograms comparing laminar distribution patterns of 5-HT binding sites in inferior frontal gyrus. For general figure information see legend to Figure 1.

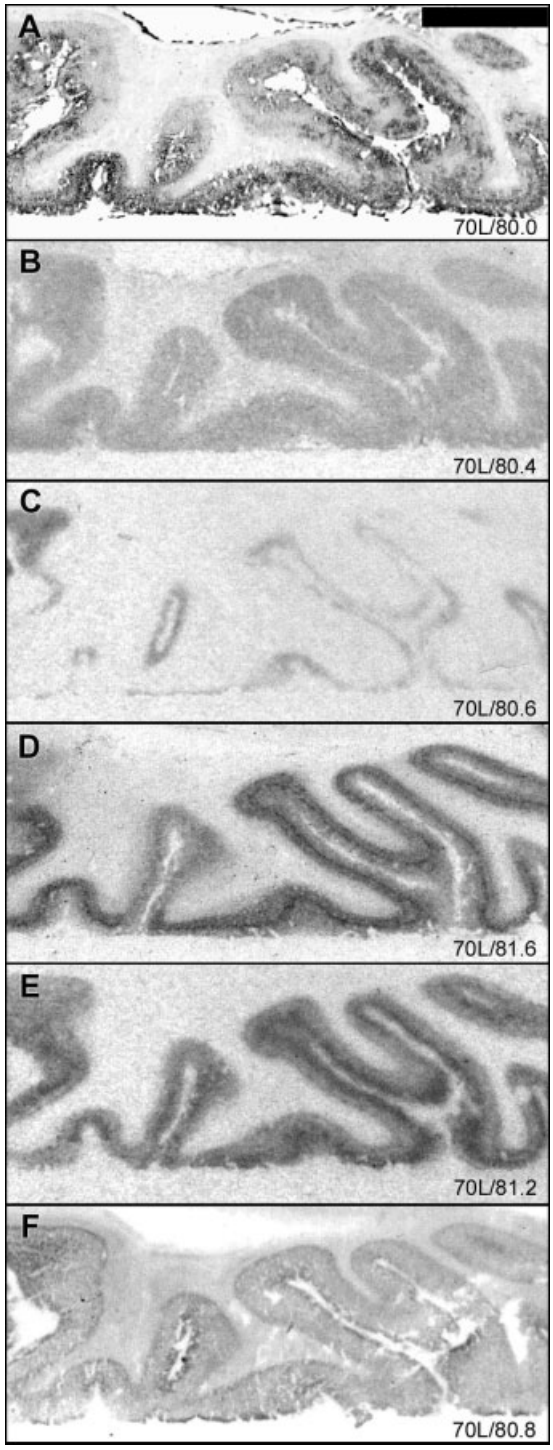

Figure 6.
Autoradiograms illustrating distribution patterns of 5-HT binding sites in occipital cortex. For general figure information see legend to Figure 1.

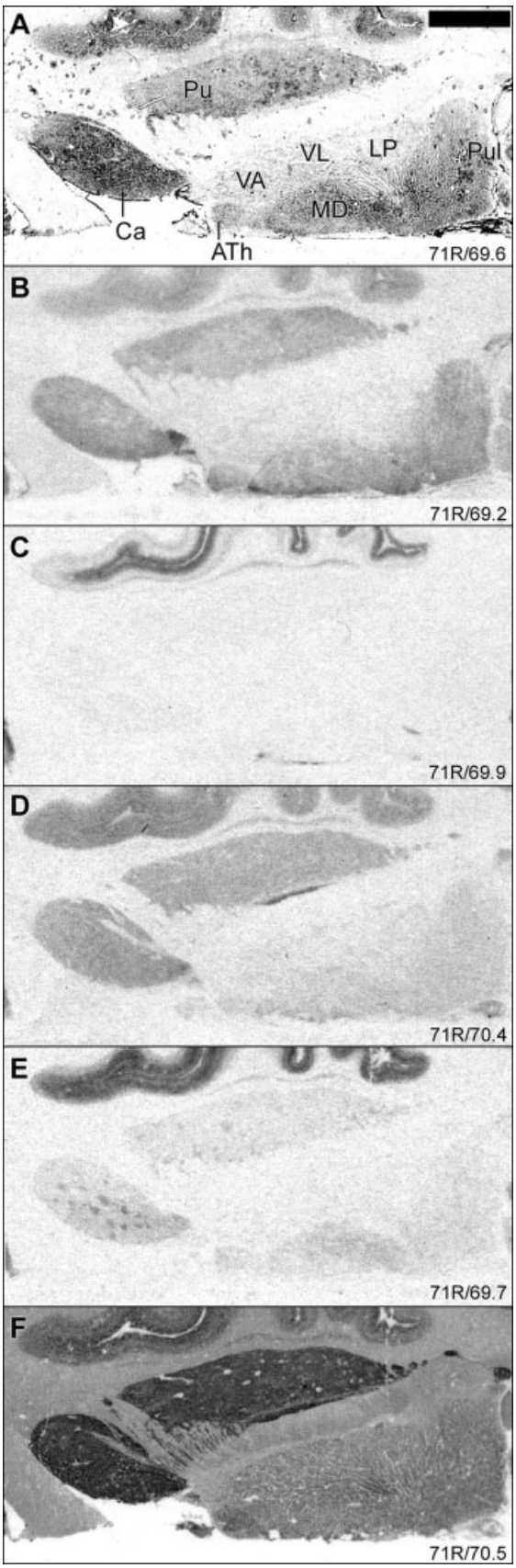

clei, whereas [^{3}H]WAY-100635 binding was concentrated to the dorsal and median raphe nuclei and [^{3}H]M100907 binding densities were low to absent in the brainstem at the levels studied. High levels of [^{3}H]GR 125743 binding and comparatively high [^{125}I]SB 207710 binding sites were observed in substantia nigra, with lower levels of [^{3}H]citalopram binding sites (Fig. 1, 2). All binding sites were low to absent in the red nucleus (Fig. 2). In the central gray area including the dorsal raphe nucleus, high levels of [^{3}H]citalopram binding, intermediately high [^{3}H]GR 125743 binding, and very low levels of [^{125}I]SB 207710 binding sites were detected. In a midline structure, probably corresponding to the interpeduncular nucleus, high levels of [^{3}H]citalopram binding, moderate levels of [^{3}H]GR 125743 and [^{125}I]SB 207710 binding sites, and low levels of [^{3}H]WAY-100635 binding sites were observed (Fig. 8). [^{3}H]Citalopram binding was very high and [^{3}H]GR 125743 binding was relatively high in the inferior colliculus, whereas binding to the other receptors was low to absent in this region (Fig. 8).

The locus coeruleus showed dense [^{3}H]citalopram binding and very low levels of [^{3}H]WAY-100635 binding with no clear evidence for specific binding to the other 5-HT receptors. [^{3}H]GR 125743 and [^{125}I]SB 207710 binding sites were also detected in the locus coeruleus, although the level of nonspecific binding was high in this region. Low levels of [^{3}H]citalopram and [^{125}I]SB 207710 binding were identified in pontine nuclei (Fig. 4).

In the cerebellar cortex, specific binding was low to absent for all the examined binding sites (Fig. 4, 8). [^{3}H]Citalopram binding was concentrated in a band probably corresponding to the Purkinje cell layer.

Other Regions

Evidence for high levels of [^{3}H]citalopram binding, relatively high levels of [^{3}H]GR 125743 binding, and very low levels of [^{3}H]WAY-100635 and [^{125}I]SB 207710 binding sites was found in septal nuclei (results not shown). [^{3}H]Citalopram binding densities were high in the bed nucleus of stria terminalis where lower levels of [^{3}H]GR 125743 and [^{125}I]SB 207710 binding sites were detected (Fig. 7). Dense [^{3}H]citalopram binding was observed in parts of the olfactory tract. Other binding sites were low to absent in this structure (results not shown). The levels of 5-HT binding sites examined were low to absent in the subthalamic nucleus.

DISCUSSION

Previous studies have described the distribution of different 5-HT binding sites in the human brain. The present study, however, allowed mapping and comparison of 5-HT receptors and the 5-HT transporter in adjacent sections of human brains. Qualitatively, the use of adjacent brain sec-

Figure 7.
Autoradiographic distribution of 5-HT binding sites in striatum and thalamus. For general figure information see legend to Figure 1.

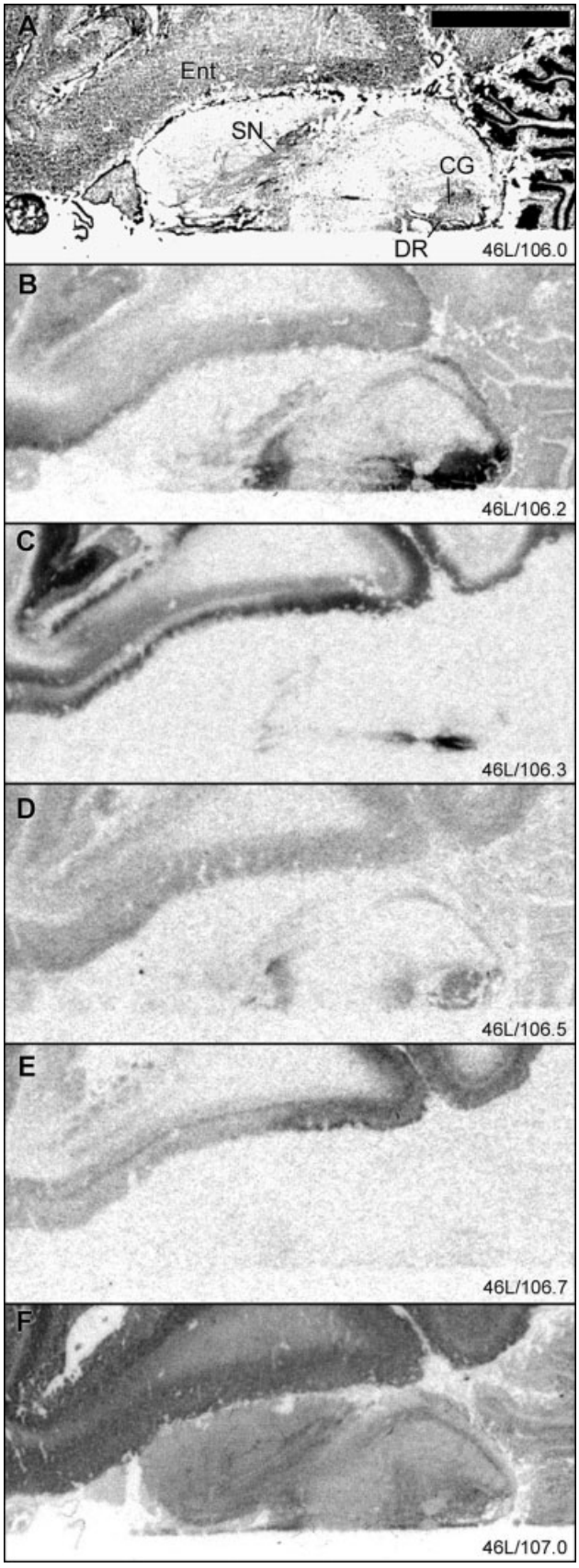

tions and radioligands for several 5-HT binding sites give support for the subregional colocalization/compartmentalization of different receptor subtypes. This study provides high-resolution anatomic correlates for lower resolution in vivo neuroimaging studies of the 5-HT system.

There were only a small number of subjects, as whole hemisphere brain tissue is not easily available. Tissue from only one female brain was included, and there was a large variation in postmortem interval. Furthermore, lateralization of receptor densities as has been indicated for the 5-HT_{2A} receptor [Rosel et al., 2002] may occur. These factors may possibly have influenced the densities and increased data variance.

In general, our results are in agreement with previous autoradiographic studies of 5-HT receptors in the human brain [Hall et al., 1997, 2000; Pazos et al., 1987a,b; Varnäs et al., 2001]. The levels of 5-HT transporters, however, were markedly lower in substantia nigra in the present study compared to that in previous analyses [Chinaglia et al., 1993; Cortés et al., 1988; Gurevich and Joyce, 1996]. The reason for this discrepancy is not clear, but could possibly be due to different subregions examined. Also 5-HT_{1B} receptor densities in the hippocampus were markedly lower compared to that in a previous study using [^{3}H]alniditan as a radioligand [Bonaventure et al., 1997]. Our data indicate high levels of 5-HT_{1A} receptors in the subcallosal area compared to that in other frontal cortical regions. This is in contrast to results obtained using the 5-HT_{1A} agonist radioligand [^{3}H]8-OH-DPAT [Pazos et al., 1987b]. The density of 5-HT_4 receptors was markedly lower compared to that in previous studies using tritiated radioligands [Bonaventure et al., 2000; Reynolds et al., 1995]. It should be noted, however, that the [^{125}I]SB 207710 concentration used in the present study was about fivefold lower than reported K_D values for this radioligand [Brown et al., 1993; Kaumann et al., 1995]. The calculated B_{max} values are thus in line with the data by Reynolds et al. [1995], although Bonaventure et al. [2000] reported approximately tenfold higher densities using the 5-HT_4 receptor radioligand [^{3}H]R116712. For instance, given the K_D value of 86 pM as reported for the piglet hippocampus [Brown et al., 1993], transformation of our data would give a B_{max} value of approximately 2 in the hippocampus, which is similar to densities presented by Reynolds et al. [1995]. The reason for the discrepant results obtained using different 5-HT_4 receptor radioligands is not clear.

Due to limited selectivity of the available pharmacologic tools for human 5-HT_{1B} and 5-HT_{1D} receptor subtypes, these are not easily distinguished [see Hoyer et al., 2002]. In this study, we used the nonselective 5-$HT_{1B/1D}$ receptor radioligand [^{3}H]GR 125743 in the presence of the recently developed compound, PNU-142633, which shows more than 3000-fold selectivity for 5-HT_{1D} versus 5-HT_{1B} receptors

Figure 8.
Autoradiographic distribution of 5-HT binding sites in brainstem. For general figure information see legend to Figure 1.

[McCall et al., 2002], to selectively label 5-HT_{1B} receptor subtypes.

Our characterization extends previous findings [Gurevich and Joyce, 1996; Mantere et al., 2002] that 5-HT transporters are highly abundant in several regions of the limbic lobe as defined by Heimer [2003]. Densities of 5-HT transporters thus were markedly higher compared to that in isocortex in regions such as anterior cingulate, subcallosal area, posterior uncus, entorhinal and insular cortices, and the temporal pole. Based on cortical development and regional architecture, these regions are referred to as the greater limbic lobe, according to the definition by Heimer [2003]. The high density of 5-HT transporters in these regions is in line with the documented role for 5-HT in the modulation of mood and emotion [Young and Leyton, 2002], and the involvement of the 5-HT transporter in the pharmacologic treatment of several psychiatric disorders.

In cingulate gyrus, the 5-HT transporter binding sites displayed lowest binding in the posterior parts, higher in anterior cingulate gyrus, and highest in the subcallosal area, where high densities of 5-HT_{1A} receptors were also observed. Anterior and ventral regions of cingulate gyrus are suggested to be involved in affect regulation [see Vogt et al., 1997], and abnormal activity and reduced cortical volume in the subcallosal area has been reported in the brain of depressed patients [Drevets et al., 1997]. The subcallosal area is activated during sadness in control subjects and activity in this region seems to be reduced with recovery from depression [Mayberg et al., 1999]. The high levels of 5-HT transporters and 5-HT_{1A} receptors in the subcallosal area may indicate that these sites are main targets in the pharmacologic treatment of depression.

In the hippocampal formation, 5-HT transporter binding was higher in the molecular layer compared to that in the pyramidal cell layer, and was higher in CA3 and external layers of subiculum compared to that in CA1–2. Receptor binding sites, in general, were highest in regions of CA1–2, with low to very low levels in CA3. Binding to the 5-HT_{1A} receptor was highest in pyramidal layers of CA1–2 and lower in the molecular layers of the Ammon's horn. To the best of our knowledge, a detailed cytoarchitectonic characterization of 5-HT_{1B} receptors in the human hippocampal formation has not yet been carried out. In a previous study [Varnäs et al., 2001], which did not attempt to analyze the layer specific distribution in detail, we proposed that 5-HT_{1B} receptors are localized in an inner part of the pyramidal cell layer. The resolution of whole hemisphere autoradiography does not allow a detailed microanatomic analysis at the cellular level. The more detailed analysis carried out in this study using adjacent sections, however, suggests that 5-HT_{1B} receptors are localized in the molecular cell layer (lacunosum moleculare), where 5-HT_{1A} and the 5-HT transporter are also localized.

5-HT has been shown to be implicated in cognition and some effects have been ascribed to modulation of hippocampal activity [Buhot, 1997]. Different receptors may be involved in different aspects of cognitive function and may even act in the opposite direction. The 5-HT_{1A} agonist 8-OH-DPAT impairs spatial memory in rats [for review, see Buhot, 1997]. A recent clinical study demonstrated that hippocampal 5-HT_{1A} receptor binding, as measured with PET, correlates negatively with explicit memory function [Yasuno et al., 2003]. Concerning the 5-HT_{1B} receptor subtype, intrahippocampal injection of a 5-HT_{1B} agonist impaired reference memory in rats [Buhot et al., 1995]. Less is known about the involvement of the human 5-HT_{1B} receptors in learning and memory. The present findings, indicating relatively low levels of 5-HT_{1B} receptor densities in the human hippocampal formation, particularly compared to the very abundant 5-HT_{1A} receptor, may suggest that the direct effects of this receptor subtype on hippocampal function are more limited in the human brain. As 5-HT_{1B} receptors, however, are localized abundantly in septal nuclei of human brain, these may indirectly modulate hippocampal activity.

The densities of 5-HT binding sites were heterogeneous in the striatum, but with different subregional distribution patterns. In caudate nucleus, binding to the 5-HT transporter was higher in medial parts. A somewhat similar regional distribution pattern with high densities in medial caudate nucleus has been reported previously for the dopamine D_1 receptor [Hall et al., 1994]. The levels of 5-HT transporter binding sites were also higher in the medial part of ventral striatum, probably corresponding to parts of the shell region.

In interpeduncular nucleus, very high levels of 5-HT transporters and relatively high levels of 5-HT_{1B} receptors were detected. Low levels of 5-HT_{1A} and 5-HT_4 receptor binding sites were found also in this nucleus. The localization of 5-HT_{1B} receptors in the interpeduncular nucleus is in agreement with findings of these binding sites in other species [Waeber et al., 1990]. Very high levels of 5-HT_4 receptor binding sites are present in the interpeduncular nucleus of the rat brain [Waeber et al., 1994]. Species differences have been demonstrated with much lower levels in the guinea pig compared to that in the rat interpeduncular nucleus [Waeber et al., 1994]. In the present study, 5-HT_4 receptor densities in the human interpeduncular nucleus were low to intermediate, and are thus comparable to the distribution seen in the guinea pig brain.

CONCLUSION

It can be concluded that the different 5-HT receptors have unique distribution patterns in the human brain, reflecting their different functional physiologic effects. The general localization in regions belonging to limbic cortico-striato-pallido-thalamic circuits is in line with the documented role for 5-HT in the modulation of mood and emotion, and the suggested involvement of this system in the pathophysiology of various psychiatric disorders. Moreover, the specific distribution pattern is the basis for modulation of selected 5-HT receptor pathways when treating different psychiatric disorders.

ACKNOWLEDGMENTS

We thank Ms. K. Larsson, Mr. D. Card, Ms. S. Eriksson, and Dr. R.S. Mulligan for their excellent technical assistance, and Professor L. Heimer and Professor Y.L. Hurd for excellent discussions on neuroanatomy. We also thank Ms. P. Flodby for assistance with the preparation of the article. A portion of the data has been presented at the 11th AEP congress in Stockholm, May 2002.

REFERENCES

Arango V, Underwood MD, Gubbi AV, Mann JJ (1995): Localized alterations in pre- and postsynaptic serotonin binding sites in the ventrolateral prefrontal cortex of suicide victims. Brain Res 688: 121–133.

Arango V, Underwood MD, Mann JJ (1997): Postmortem findings in suicide victims. Implications for in vivo imaging studies. Ann N Y Acad Sci 836:269–287.

Artigas F, Romero L, de Montigny C, Blier P (1996): Acceleration of the effect of selected antidepressant drugs in major depression by 5-HT_{1A} antagonists. Trends Neurosci 19:378–383.

Bantick RA, Deakin JF, Grasby PM (2001): The 5-HT_{1A} receptor in schizophrenia: a promising target for novel atypical neuroleptics? J Psychopharmacol 15:37–46.

Baumgarten HG, Grozdanovic Z (1997): Anatomy of central serotoninergic projection systems. In: Baumgarten HG, Göthert M, editors. Serotoninergic neurons and 5-HT receptors in the CNS. Berlin: Springer-Verlag. p 41-89.

Bonaventure P, Hall H, Gommeren W, Cras P, Langlois X, Jurzak M, Leysen JE (2000): Mapping of serotonin 5–HT_4 receptor mRNA and ligand binding sites in the post-mortem human brain. Synapse 36:35–46.

Bonaventure P, Schotte A, Cras P, Leysen JE (1997): Autoradiographic mapping of 5-HT_{1B}- and 5-HT_{1D} receptors in human brain using [^{3}H]alniditan, a new radioligand. Receptors Channels 5:225–230.

Brown AM, Young TJ, Patch TL, Cheung CW, Kaumann AJ, Gaster L, King FD (1993): [^{125}I]-SB 207710, a potent, selective radioligand for 5-HT_4 receptors. Br J Pharmacol 110:10P.

Buhot MC (1997): Serotonin receptors in cognitive behaviors. Curr Opin Neurobiol 7:243–254.

Buhot MC, Patra SK, Naïli S (1995): Spatial memory deficits following stimulation of hippocampal 5-HT_{1B} receptors in the rat. Eur J Pharmacol 285:221–228.

Chinaglia G, Landwehrmeyer B, Probst A, Palacios JM (1993): Serotoninergic terminal transporters are differentially affected in Parkinson's disease and progressive supranuclear palsy: an autoradiographic study with [^{3}H]citalopram. Neuroscience 54:691–699.

Cortés R, Soriano E, Pazos A, Probst A, Palacios JM (1988): Autoradiography of antidepressant binding sites in the human brain: localization using [^{3}H]imipramine and [^{3}H]paroxetine. Neuroscience 27:473–496.

Crabbe JC, Phillips TJ, Feller DJ, Hen R, Wenger CD, Lessov CN, Schafer GL (1996): Elevated alcohol consumption in null mutant mice lacking 5-HT_{1B} serotonin receptors. Nat Genet 14:98–101.

Dean B (2003): The cortical serotonin$_{2A}$ receptor and the pathology of schizophrenia: a likely accomplice. J Neurochem 85:1–13.

Doménech T, Beleta J, Palacios JM (1997): Characterization of human serotonin 1D and 1B receptors using [^{3}H]-GR-125743, a novel radiolabelled serotonin 5HT1D/1B receptor antagonist. Naunyn Schmiedebergs Arch Pharmacol 356:328–334.

Drevets WC, Frank E, Price JC, Kupfer DJ, Holt D, Greer PJ, Huang Y, Gautier C, Mathis C (1999): PET imaging of serotonin 1A receptor binding in depression. Biol Psychiatry 46:1375–1387.

Drevets WC, Price JL, Simpson JR Jr, Todd RD, Reich T, Vannier M, Raichle ME (1997): Subgenual prefrontal cortex abnormalities in mood disorders. Nature 386:824–827.

Eglen RM (1997): 5-Hydroxytryptamine (5-HT)$_4$ receptors and central nervous system function: an update. Prog Drug Res 49:9–24.

Gurevich EV, Joyce JN (1996): Comparison of [^{3}H]paroxetine and [^{3}H]cyanoimipramine for quantitative measurement of serotonin transporter sites in human brain. Neuropsychopharmacology 14:309–323.

Hall H, Sedvall G, Magnusson O, Kopp J, Halldin C, Farde L (1994): Distribution of D_1- and D_2-dopamine receptors, and dopamine and its metabolites in the human brain. Neuropsychopharmacology 11:245–256.

Hall H, Farde L, Halldin C, Lundkvist C, Sedvall G (2000): Autoradiographic localization of 5-HT_{2A} receptors in the human brain using [^{3}H]M100907 and [^{11}C]M100907. Synapse 38:421–431.

Hall H, Halldin C, Farde L, Sedvall G (1998): Whole hemisphere autoradiography of the postmortem human brain. Nucl Med Biol 25:715–719.

Hall H, Hurd Y, Pauli S, Halldin C, Sedvall G (2001): Human brain imaging post-mortem—whole hemisphere technologies. Int Rev Psychiatry 13:12–17.

Hall H, Lundkvist C, Halldin C, Farde L, Pike VW, McCarron JA, Fletcher A, Cliffe IA, Barf T, Wikström H, Sedvall G (1997): Autoradiographic localization of 5-HT_{1A} receptors in the postmortem human brain using [^{3}H]WAY-100635 and [^{11}C]WAY-100635. Brain Res 745:96–108.

Heimer L (2003): A new anatomical framework for neuropsychiatric disorders and drug abuse. Am J Psychiatry 160:1726–1739.

Hoyer D, Hannon JP, Martin GR (2002): Molecular, pharmacological and functional diversity of 5-HT receptors. Pharmacol Biochem Behav 71:533–554.

Ito H, Nyberg S, Halldin C, Lundkvist C, Farde L (1998): PET imaging of central 5-HT_{2A} receptors with carbon-11-MDL 100,907. J Nucl Med 39:208–214.

Kaumann AJ, Lynham JA, Brown AM (1995): Labelling with [^{125}I]-SB 207710 of a small 5-HT_4 receptor population in piglet right atrium: functional relevance. Br J Pharmacol 115:933–936.

Kehne JH, Baron BM, Carr AA, Chaney SF, Elands J, Feldman DJ, Frank RA, van Giersbergen PL, McCloskey TC, Johnson MP, McCarty DR, Poirot M, Senyah Y, Siegel BW, Widmaier C (1996): Preclinical characterization of the potential of the putative atypical antipsychotic MDL 100,907 as a potent 5-HT_{2A} antagonist with a favorable CNS safety profile. J Pharmacol Exp Ther 277:968–981.

Khawaja X, Evans N, Reilly Y, Ennis C, Minchin MC (1995): Characterisation of the binding of [^{3}H]WAY-100635, a novel 5-hydroxytryptamine1A receptor antagonist, to rat brain. J Neurochem 64:2716–2726.

López-Giménez JF, Mengod G, Palacios JM, Vilaró MT (1999): Human striosomes are enriched in 5-HT_{2A} receptors: autoradiographical visualization with [^{3}H]MDL100,907, [^{125}I](+/−)DOI and [^{3}H]ketanserin. Eur J Neurosci 11:3761–3765.

Malison RT, Price LH, Berman R, van Dyck CH, Pelton GH, Carpenter L, Sanacora G, Owens MJ, Nemeroff CB, Rajeevan N, Baldwin RM, Seibyl JP, Innis RB, Charney DS (1998): Reduced brain serotonin transporter availability in major depression as measured by [^{123}I]-2β-carbomethoxy-3β-(4-iodophenyl)tropane and single photon emission computed tomography. Biol Psychiatry 44:1090–1098.

Mantere T, Tupala E, Hall H, Särkioja T, Räsänen P, Bergström K, Callaway J, Tiihonen J (2002): Serotonin transporter distribution and density in the cerebral cortex of alcoholic and nonalcoholic comparison subjects: a whole-hemisphere autoradiography study. Am J Psychiatry 159:599–606.

Mayberg HS, Liotti M, Brannan SK, McGinnis S, Mahurin RK, Jerabek PA, Silva JA, Tekell JL, Martin CC, Lancaster JL, Fox PT (1999): Reciprocal limbic-cortical function and negative mood: converging PET findings in depression and normal sadness. Am J Psychiatry 156:675–682.

McCall RB, Huff R, Chio CL, TenBrink R, Bergh CL, Ennis MD, Ghazal NB, Hoffman RL, Meisheri K, Higdon NR, Hall E (2002): Preclinical studies characterizing the anti-migraine and cardiovascular effects of the selective 5-HTID receptor agonist PNU-142633. Cephalalgia 22:799–806.

Meltzer HY, Matsubara S, Lee JC (1989): Classification of typical and atypical antipsychotic drugs on the basis of dopamine D-1, D-2 and serotonin2 pKi values. J Pharmacol Exp Ther 251:238–246.

Moret C, Briley M (2000): The possible role of 5-$HT_{1B/D}$ receptors in psychiatric disorders and their potential as a target for therapy. Eur J Pharmacol 404:1–12.

Nutt DJ, Forshall S, Bell C, Rich A, Sandford J, Nash J, Argyropoulos S (1999): Mechanisms of action of selective serotonin reuptake inhibitors in the treatment of psychiatric disorders. Eur Neuropsychopharmacol 9(Suppl.):81–86.

Österlund MK, Halldin C, Hurd YL (2000): Effects of chronic 17β-estradiol treatment on the serotonin 5-HT_{1A} receptor mRNA and binding levels in the rat brain. Synapse 35:39–44.

Patel S, Roberts J, Moorman J, Reavill C (1995): Localization of serotonin-4 receptors in the striatonigral pathway in rat brain. Neuroscience 69:1159–1167.

Pazos A, Probst A, Palacios JM (1987a): Serotonin receptors in the human brain—IV. Autoradiographic mapping of serotonin-2 receptors. Neuroscience 21:123–139.

Pazos A, Probst A, Palacios JM (1987b): Serotonin receptors in the human brain—III. Autoradiographic mapping of serotonin-1 receptors. Neuroscience 21:97–122.

Pike VW, Halldin C, Nobuhara K, Hiltunen J, Mulligan RS, Swahn CG, Karlsson P, Olsson H, Hume SP, Hirani E, Whalley J, Pilowsky LS, Larsson S, Schnell PO, Ell PJ, Farde L (2003): Radioiodinated SB 207710 as a radioligand in vivo: imaging of brain 5-HT_4 receptors with SPET. Eur J Nucl Med Mol Imaging 30:1520–1528.

Pike VW, McCarron JA, Lammertsma AA, Osman S, Hume SP, Sargent PA, Bench CJ, Cliffe IA, Fletcher A, Grasby PM (1996): Exquisite delineation of 5-HT_{1A} receptors in human brain with PET and [carbonyl-^{11} C]WAY-100635. Eur J Pharmacol 301:5–7.

Reynolds GP, Mason SL, Meldrum A, De Keczer S, Parnes H, Eglen RM, Wong EH (1995): 5-Hydroxytryptamine (5-HT)$_4$ receptors in post mortem human brain tissue: distribution, pharmacology and effects of neurodegenerative diseases. Br J Pharmacol 114: 993–998.

Rocha BA, Scearce-Levie K, Lucas JJ, Hiroi N, Castanon N, Crabbe JC, Nestler EJ, Hen R (1998): Increased vulnerability to cocaine in mice lacking the serotonin-1B receptor. Nature 393:175–178.

Rosel P, Arranz B, Urretavizcaya M, Oros M, San L, Vallejo J, Navarro MA (2002): Different distributions of the 5-HT reuptake complex and the postsynaptic 5-HT_{2A} receptors in Brodmann areas and brain hemispheres. Psychiatry Res 111:105–115.

Sargent PA, Kjaer KH, Bench CJ, Rabiner EA, Messa C, Meyer J, Gunn RN, Grasby PM, Cowen PJ (2000): Brain serotonin$_{1A}$ receptor binding measured by positron emission tomography with [^{11}C]WAY-100635: effects of depression and antidepressant treatment. Arch Gen Psychiatry 57:174–180.

Saudou F, Aït Amara D, Dierich A, LeMeur M, Ramboz S, Segu L, Buhot MC, Hen R (1994): Enhanced aggressive behavior in mice lacking 5-HT_{1B} receptor. Science 265:1875–1878.

Sramek JJ, Zarotsky V, Cutler NR (2002): Generalised anxiety disorder: treatment options. Drugs 62:1635–1648.

Szabo Z, Kao PF, Scheffel U, Suehiro M, Mathews WB, Ravert HT, Musachio JL, Marenco S, Kim SE, Ricaurte GA, et al. (1995): Positron emission tomography imaging of serotonin transporters in the human brain using [^{11}C](+)McN5652. Synapse 20:37–43.

Tauscher J, Kapur S, Verhoeff NP, Hussey DF, Daskalakis ZJ, Tauscher-Wisniewski S, Wilson AA, Houle S, Kasper S, Zipursky RB (2002): Brain serotonin 5-HT_{1A} receptor binding in schizophrenia measured by positron emission tomography and [^{11}C]WAY-100635. Arch Gen Psychiatry 59:514–520.

Waeber C, Palacios JM (1994): Binding sites for 5-hydroxytryptamine-2 receptor agonists are predominantly located in striosomes in the human basal ganglia. Brain Res Mol Brain Res 24:199–209.

Waeber C, Schoeffter P, Hoyer D, Palacios JM (1990): The serotonin 5-HT_{1D} receptor: a progress review. Neurochem Res 15:567–582.

Waeber C, Sebben M, Nieoullon A, Bockaert J, Dumuis A (1994): Regional distribution and ontogeny of 5-HT_4 binding sites in rodent brain. Neuropharmacology 33:527–541.

Varnäs K, Hall H, Bonaventure P, Sedvall G (2001): Autoradiographic mapping of 5-HT_{1B} and 5-HT_{1D} receptors in the post mortem human brain using [^{3}H]GR 125743. Brain Res 915:47–57.

Varnäs K, Halldin C, Pike VW, Hall H (2003): Distribution of 5-HT_4 receptors in the postmortem human brain - an autoradiographic study using [^{125}I]SB 207710. Eur Neuropsychopharmacol 13:228–234.

Vogt BA, Vogt LJ, Nimchinsky EA, Hof PR (1997): Primate cingulate cortex chemoarchitecture and its disruption in Alzheimer's disease. In: Bloom FE, Björklund A, Hökfelt T, editors. Handbook of chemical neuroanatomy. Amersterdam: Elsevier Science BV. p 455–528.

Yasuno F, Suhara T, Nakayama T, Ichimiya T, Okubo Y, Takano A, Ando T, Inoue M, Maeda J, Suzuki K (2003): Inhibitory effect of hippocampal 5-HT_{1A} receptors on human explicit memory. Am J Psychiatry 160:334–340.

Young SN, Leyton M (2002): The role of serotonin in human mood and social interaction. Insight from altered tryptophan levels. Pharmacol Biochem Behav 71:857–865.